Journal of Alloys and Compounds 513 (2012) 449–454

Contents lists available at SciVerse ScienceDirect

Journal of Alloys and Compounds

journal homepage: www.elsevier.com/locate/jallcom

Comparative study on structure, corrosion and hardness of Zn–Ni alloy deposition on AISI 347 steel aircraft material

RM. Gnanamuthu[a], S. Mohan[b,*], G. Saravanan[b], Chang Woo Lee[a,*]

[a] Department of Chemical Engineering, College of Engineering, Kyung Hee University, 1732 Deogyeong-daero, Gihung, Yongin, Gyeonggi 446-701, South Korea
[b] Central Electrochemical Research Institute, (CSIR), Karaikudi 630 006, Tamilnadu, India

ARTICLE INFO

Article history:
Received 23 August 2011
Received in revised form 20 October 2011
Accepted 22 October 2011
Available online 7 November 2011

Keywords:
Metals and alloys
Corrosion: Electrochemical reactions: Pulse plating
AFM

ABSTRACT

Zn–Ni alloys were electrodeposited on AISI 347 steel aircraft materials from various electrolytes under direct current (DCD) and pulsed electrodepositing (PED) techniques. The effects of pulse duty cycle on thickness, current efficiency and hardness of electrodeposits were studied. Alloy phases of the Zn–Ni were indexed by X-ray diffraction (XRD) techniques. Microstructural morphology, topography and elemental compositions were characterized using scanning electron microscopy (SEM), atomic force microscopy (AFM) and X-ray fluorescence spectroscopy (XRF). The corrosion resistance properties of electrodeposited Zn–Ni alloy in 3.5% NaCl aqueous solution obtained by DCD and PED were compared using potentiodynamic polarization and electrochemical impedance spectroscopy (EIS) technique. Elemental analysis showed that 88% of Zn and 12% of Ni obtained from electrolyte-4 by PED technique at 40% duty cycle for 50 Hz frequencies having better corrosion resistance than that of deposits obtained from other electrolytes.

1. Introduction

Electrodeposited Zn–Ni alloy provides an excellent corrosion resistance for steel in relatively aggressive environments. Recently Zn–Ni alloys have received more interest than other alloys [1,2] because of more negative than Fe and dissolve rapidly in highly corrosive environments. Nickel-based alloys are used in a wide variety of applications for aerospace, energy generation and corrosion protection, especially in an environment where materials have to withstand high temperatures and oxidizing conditions. Zn–Ni alloy electrodeposition was carried out in a sulfamate bath by pulse plating [3]. Zn–Ni alloy coatings were carried out by direct current (DC), pulse current (PC) and pulse reverse current (PRC) methods in a sulfate bath [4]. Ramanauskas et al. studied the effects of the pulse parameters on the surface morphology, grain size and corrosion properties of Zn–Ni alloy coatings. Compared with coatings deposited by DC plating, the grain size became smaller, the coating surface became denser and smoother, the crystal grains evenly distributed and the number of lattice lacuna also increased, which led to the improvement of the corrosion resistance in a ZnO bath [5]. The structure morphology of electrodeposited Zn–Ni alloy is fine grained than that of a Zn electrodeposits. A nanocrystalline Zn–Ni coating can be obtained from an ammonium chloride and chloride based electrolytes [6,7]. Although alkaline Zn–Ni electroplating has been successfully developed, there are no unambiguous reports regarding the nanocrystalline Zn–Ni coating obtained from an alkaline bath. Particularly Zn–Ni alloys owing to their excellent corrosion resistance behaviour in saline environments.

The mechanism for electrodeposition of Zn–Ni alloys in NH_4Cl electrolyte is the formation of mixed intermediate surface compound ($ZnNi^+_{ads}$) adsorbed at cathode surface is shown in Eq. (2) [8].

$$(ZnNi^+_{ads}) + e^- \rightarrow Zn + Ni \quad (1)$$

Also, Hadian and Gabe reported that pulse plating mode could reduce the residual stress of the alloy coatings in a certain degree [9]. The properties of alloy coatings greatly depend on the structure and the composition [10]. Due to be favor of resolving many problems of the direct current (DC) plating, these techniques present the promising prospects in the inexpensive metal plating field [11]. However, there are only a few instances of the research on Zn–Ni alloy coating by PC and PRC plating technique reported at present. The present work demonstrates the structure, hardness and corrosion properties of Zn–Ni alloy and Zn on AISI 347 stainless steel aircraft materials under direct and pulsed current techniques using various electrolytes.

* Corresponding authors. Tel.: +82 31 201 3825; fax: +82 31 204 8114.
E-mail addresses: sanjnamohan@yahoo.com (S. Mohan), cwlee@khu.ac.kr (C.W. Lee).

0925-8388/$ – see front matter © 2011 Elsevier B.V. All rights reserved.
doi:10.1016/j.jallcom.2011.10.078

Table 1
The used electrolytes for Zn–Ni alloy and conventional Zn on AISI 347 stainless steel by DCD and PED process.

Electrolyte Number	Electrolyte composition	Concentrations, M
1	$ZnSO_4$: NH_4Cl: NH_4SO_4: SLS brightener: Saccharin	0.83: 0.28: 0.22: 0.01:0.05
2	$ZnCl_2$: $NiCl_2$: KCl: NH_4Cl: H_3BO_3: SLS: Saccharin	0.5: 0.25: 2.0: 1.0: 0.5: 0.01:0.05
3	$ZnSO_4$: $NiSO_4$: H_2SO_4: Na_2SO_4: H_3BO_3: SLS: Saccharin	0.20: 0.20: 0.01: 0.04: 0.16: 0.01
4	$ZnSO_4$: $NiCl_2$: HCHO: CH_3COOH: SLS: Saccharin	1.0: 0.84: 0.16: 0.5: 0.01: 0.05

2. Experimental details

2.1. Preparation of electrolytes and electrodeposition methods

Electrodepositions of Zn–Ni alloy were performed using various electrolytes as listed in Table 1. The conventional Zn is obtained from electrolyte-1 and Zn–Ni alloy is from electrolyte-2, 3, and 4. AR-grade chemicals and double distilled water were used to prepare the electrolytes. The temperatures of electrolytes were kept constant at 50 °C for all experiments. All electrolytes were maintained at pH ranged at 2.5; all measured at 50 °C. According to measurements made using a Testronics 511 digital pH meter. The pretreatment of AISI 347 stainless steel substrate was degreased in acetone, electrocleaned with an alkaline bath and etched in 10% HCl were used according to the previous literature [12]. Since it is very difficult to plate directly on stainless steel due to the presence of the passive layer, a Ni strike is generally performed before plating is executed with another metal or alloy. A Nickel strike solution consisting of $NiCl_2$ 240 g L^{-1}, HCl 83 ml L^{-1}, anode Ni and AISI 347 stainless steel is used as cathode. For deposition exposed area of the substrate is 12 cm^2 and insoluble graphite used as an anode and substrate was connected to the cathode in the plating system [13]. The Zn–Ni alloy and conventional Zn deposition was performed for 30 min (plating time) with current density of 4 A dm^{-2}. Both direct current (DCD) and pulsed current (PED) deposition were carried out using Aplab Model and Dynatronix DPR20-10-5 model. The pulse parameters are used according to the previous literature [14]. The formulas used in the pulse electrodeposition are given below in Eqs. (2)–(4).

$$\%\,\text{Duty cycle} = \frac{\text{On-time}}{\text{Off-time}} \times 100 \tag{2}$$

$$\text{Average current} = \frac{\text{On-time}}{\text{Total current} \times \text{Peak pulse current}} \tag{3}$$

$$\text{Peak current} = \frac{\text{Average current}}{\text{Duty cycle}} \times 100 \tag{4}$$

The surface morphology of both DCD and PED Zn–Ni alloy and conventional Zn were characterized by SEM using a Hitachi 3000H, elemental compositions were analyzed by XRF using HORIBA XGT-2700 model and AFM measurements were performed using PicoSPM I (Molecular Imaging, Tempe, AZ, USA) with PicoScan 2100 controller. Crystallite size and textures analysis were assessed by XRD technique using a Phillips diffractometer with Cu$K\alpha$ (2.2 kW maximum). The effect of thickness, current efficiency and hardness of Zn–Ni alloy deposits were investigated.

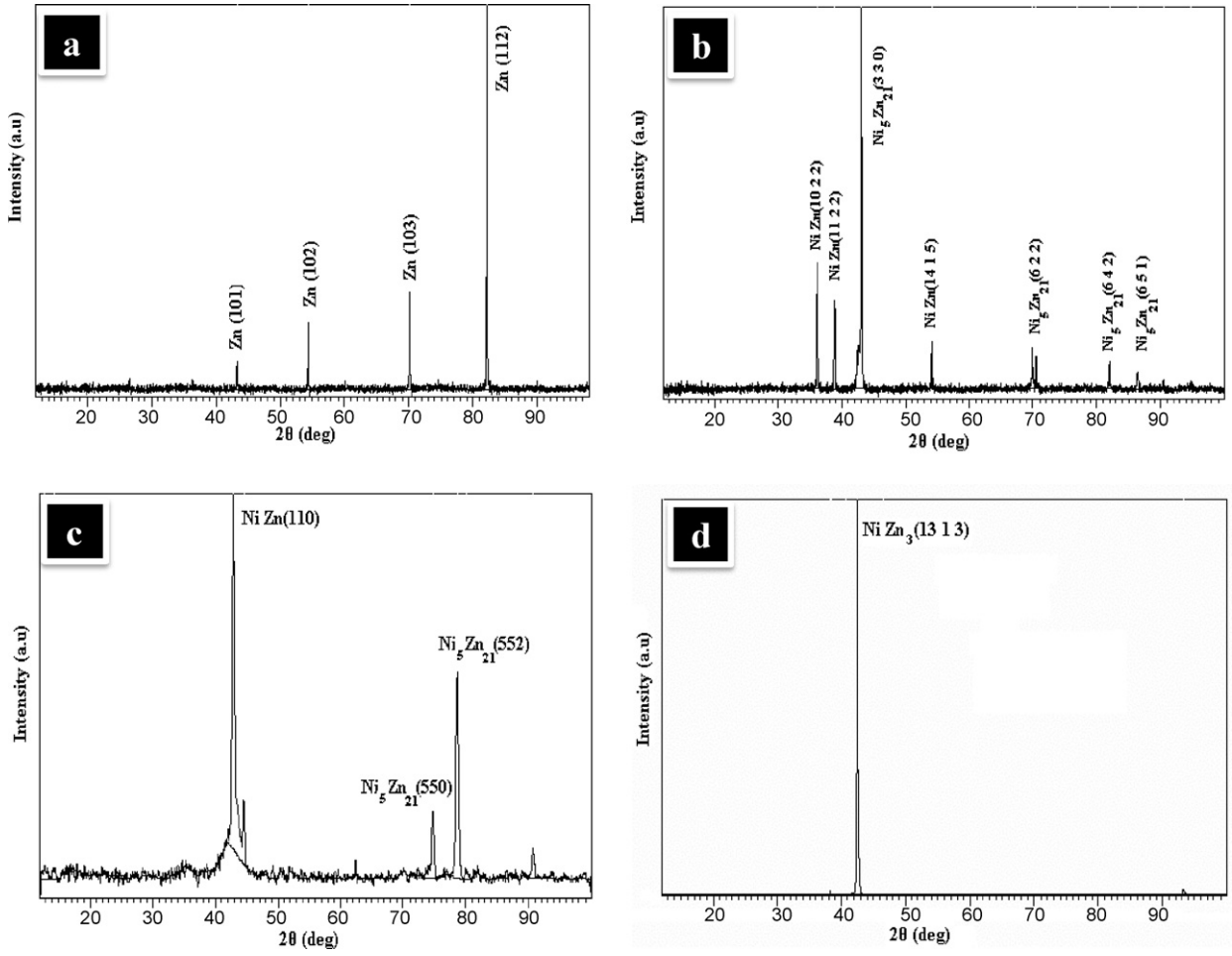

Fig. 1. XRD patterns of PED on AISI 347 stainless steel: (a) Zn electrolyte-1, (b) Zn–Ni electrolyte-2, (c) Zn–Ni electrolyte-3 and (d) Zn–Ni electrolyte-4.

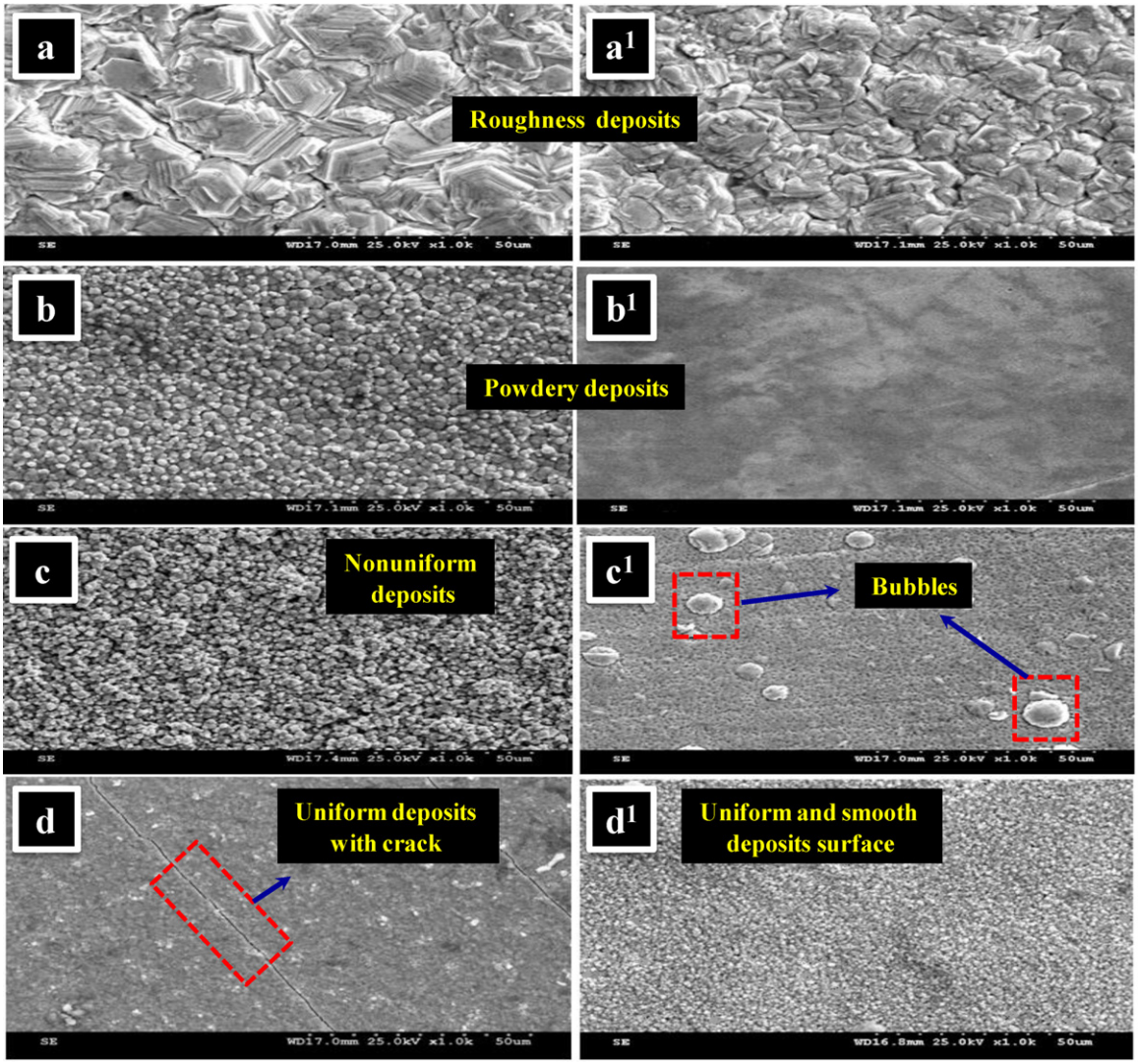

Fig. 2. SEM surface morphology of coatings; Zn electrolyte-1 by DCD (a) and PED (a^1), Zn–Ni electrolyte-2 by DCD (b) and PED (b^1), Zn–Ni electrolyte-3 by DCD (c) and PED (c^1), Zn–Ni electrolyte-4 by DCD (d) and PED (d^1).

2.2. Corrosion resistance measurements

Corrosion resistance measurements were performed using three-electrode cell with of 150 ml of 3.5% NaCl solution. The electrodeposited Zn–Ni alloy and conventional Zn on AISI 347 stainless steel substrate were used as the working electrode (WE). A platinum foil and a saturated calomel electrode (SCE) were used as the auxiliary and reference electrode, correspondingly. The electrodes were connected to a potentiostat (PARSTAT 2273). The corrosion resistance parameters were obtained with inbuilt software package (powerCORR). All potentials in this work are referred to SCE. Corrosion behaviour was examined in neutral 3.5% NaCl solution at $30 \pm 1\,^{\circ}C$. Potentiodynamic polarization curves were measured for all the samples between −1.6 and −0.6 V at a scan rate of 5 mV/s.

3. Results and discussion

3.1. Surface morphologies of the coatings

Fig. 1 shows the X-ray diffraction of the PED Zn–Ni alloy and conventional Zn on AISI 347 stainless steel from electrolytes-1–4 at current density of 4 A dm^{-2}. The electrodeposited Zn–Ni alloy on AISI 347 stainless steel from electrolyte-4 at 40% duty cycle and frequency of 50 Hz are shown in Fig. 1d. The electrodeposits consist of a strong orthorhombic $NiZn_3$ (13 1 3) plane at 2 theta = 42.5°. These alloy phases were referred to the JCPDS card (No. 47-1019) used in the analysis. The thickness of the coatings was approximately 29 μm were used in this study. The crystallite size was calculated using the Debye-Scherrer formula as shown in Eq. (5).

$$D = \frac{0.9\lambda}{\beta \cos \theta} \tag{5}$$

where D is the crystallite size, β is the FWHM, and λ is the X-ray wavelength (1.540 Å) used. The calculated crystallite size of $NiZn_3$ phases (13 1 3) is 59.7 nm which is attributed to the preferred orientation along the above plane. When the duty cycle increases, On-time increases and Off-time decreases and this leads to insufficient supply of metal ions and hence reduced nucleation rate and increased grain size during electrodeposits. Toth-Kadar et al. [15] studied coarse-grained electrodeposition due to concentration depletion occurred as On-time increased. It is found that the XRD pattern of the pulse electrodeposited Zn–Ni alloy from electrolyte-4 was better crystallinity than that of the electrolyte-1, 2, and 3.

Fig. 2 shows SEM morphologies of the Zn–Ni alloy and conventional Zn electrodeposits on AISI 347 stainless steel at current density of 4 A dm^{-2}. Fig. 2a–d, and a^1–d^1 are showed DCD and PED conventional Zn and Zn–Ni alloy correspondingly. The thickness of the coatings was approximately 29 μm were used in this study. Fig. 2d^1 shows PED Zn–Ni alloy from electrolyte-4 has a 0.5–1.5 μm grain size, which is a fine grain, and a nodular crack-free, uniformly

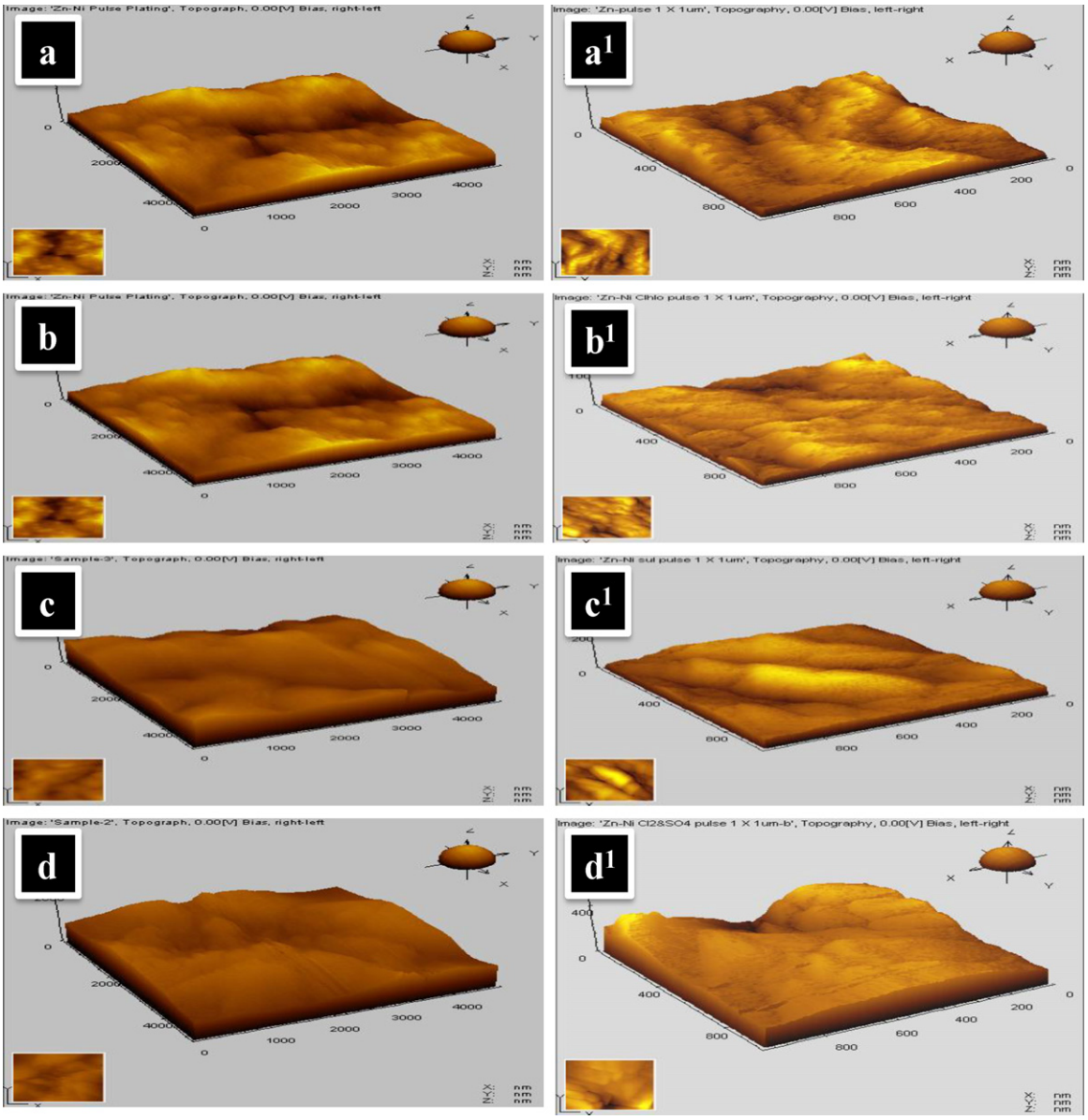

Fig. 3. Atomic force microscopy images of coatings; Zn electrolyte-1 by DCD (a) and PED (a^1), Zn–Ni electrolyte-2 by DCD (b) and PED (b^1), Zn–Ni electrolyte-3 by DCD (c) and PED (c^1), Zn–Ni electrolyte-4 by DCD (d) and PED (d^1).

smooth, bright deposit was obtained. The decreased porosity and denser packed surface are due to desorption of hydrogen during the Off-time of the pulse cycle [16]. Fig. 2d^1 shows the SEM photograph of Zn–Ni alloy deposits on AISI 347 stainless steel is obtained 88:12% ratios obtained from X-ray fluorescence studies.

Fig. 3 shows the AFM topography deposited alloy scanned over an area of 1 μm × 1 μm of the Zn–Ni alloy and conventional Zn deposits on AISI 347 stainless steel from different electrolytes at 4 A dm^{-2}. Fig. 3a–d, and a^1–d^1 are showed DCD and PED conventional Zn and Zn–Ni alloy correspondingly. Fig. 3d^1 shows Zn–Ni alloy particles by PED from electrolyte-4 have 600 nm in size obtained. Furthermore, the crystalline size reduction to the nanometer range results in considerable improvement in their corrosion resistance [17]. The surface topography of the Zn–Ni alloy obtained by PED was fine grained nodular and pores free improved structural properties from electrolyte-4 than other electrolytes.

3.2. Effect of current efficiency, thickness and hardness of Zn–Ni alloy deposits by PED

Fig. 4a shows the duty cycle on current efficiency (CE) of Zn–Ni alloy on AISI 347 stainless steel from electrolyte-4. The maximum current efficiency is obtained at 40% duty cycle and 50 Hz frequency. The pulse 40% duty cycle at lower pulse frequencies enhancement of migration of ions increases the nucleation rate, uniformity of deposit [18], and deposition rate, and hence current efficiency is increased. Higher current efficiency and thickness of deposits is obtained from electrolyte-4 than that of electrolyte-1, 2, and 3.

Fig. 4b shows the effect of pulse duty cycle on thickness of the Zn–Ni alloy deposits obtained from electrolyte-4. As the duty cycle increases, the current On-time increases but the Off-time decreases. At a lower duty cycle, the peak current is flowing for less time and the overall amount of deposition is smaller when compared with those at a higher duty cycle and frequencies. The

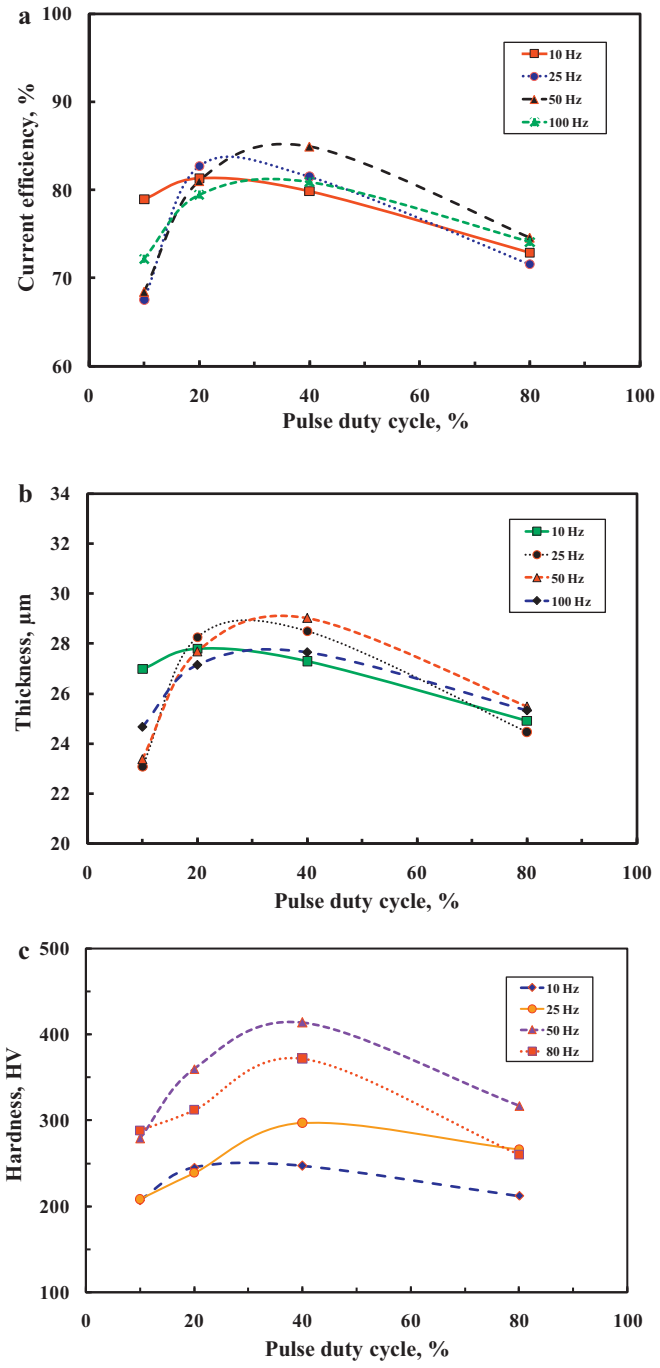

Fig. 4. Effect of pulse duty cycles on Zn–Ni alloy electrodeposits obtained at electrolyte-4: (a) current efficiency (b) thickness (c) hardness of deposits.

maximum thickness of Zn–Ni alloy on AISI 347 stainless steel was 29 μm obtained at 40% duty cycle and 50 Hz frequency.

Fig. 4c shows the effect of duty cycle on hardness of Zn–Ni alloy deposits on AISI stainless steel from electrolyte-4 was analyzed. The hardness of the Zn–Ni alloy was measured using a LECO Micro hardness tester from electrolyte-4, Zn–Ni content were analyzed by XRF and atomic absorption spectrometer (AAS) results were around 88 and 12%, respectively. A maximum hardness value of the Zn–Ni alloy was 414 HV obtained at 40% duty cycle and 50 Hz frequency. Because at low pulse duty cycle a high peak current is passed, this produces powdery or burnt deposits with poor adhesion and considerable porosity. This porosity leads to a decrease in hardness

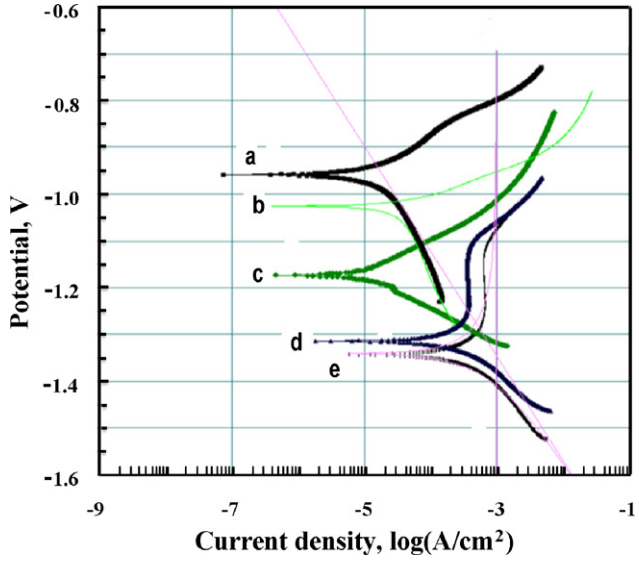

Fig. 5. Polarization studies of Zn–Ni alloy and conventional Zn deposits on AISI stainless steel in 3.5% of NaCl Solution; (a) Zn–Ni electrolyte-4 (PED), (b) Zn–Ni electrolyte-4 (DCD), (c) Zn–Ni electrolyte-3 (PED), (d) Zn–Ni electrolyte-2 (PED) and (e) Conventional Zn electrolyte-1 (PED).

Table 2
Corrosion parameters obtained from polarization studies in 3.5% NaCl solution.

Electrodeposited AISI 347 sample	E_{corr} (V)	I_{corr} (A cm^{-2})
Zn-Electrolyte-1 (PED) (e)	−1.37	1×10^{-3}
Zn–Ni-Electrolyte-2 (PED) (d)	−1.35	1×10^{-3}
Zn–Ni-Electrolyte-3 (PED) (c)	−1.15	1×10^{-4}
Zn–Ni-Electrolyte-4 (DCD) (b)	−1.02	1×10^{-4}
Zn–Ni-Electrolyte-4 (PED) (a)	−0.95	1×10^{-5}

of the deposits. Pulse plated samples have on average double the hardness of direct current plated samples [3].

3.3. Corrosion examination

Fig. 5 shows the potentiodynamic polarization curves for Zn–Ni alloy and conventional Zn electrodeposits on AISI 347 substrate using a 3.5% NaCl solution. All of the curves display active passive behaviour between −1.6 and −0.6 V. This indicates that the mechanism of activity and passivation is essentially similar for all electrodeposits. The current density increases with the increasing potential at the activation region. The electrode then passivates and displays high stability, as characterized by the low and steady value of the passive current density. The corrosion current density (I_{corr}) and corrosion potential (E_{corr}) are calculated from the intercepts of the Tafel slopes and values are given in Table 2. Among all of the samples, PED deposited (a) Zn–Ni alloy having very lower I_{corr} and high E_{corr} values than that of DCD alloy sample. Similarly for sample (b) is higher corrosion resistance than (c) which in turn higher corrosion resistance than (d). PED deposited Zn (e) is having very lower corrosion resistance than other systems. From the Corrosion parameter values Zn–Ni alloy obtained by PED deposited from electrolyte-4 having better corrosion resistance than other samples.

4. Conclusion

In this work, Zn–Ni alloy and conventional Zn obtained on AISI 347 aircraft material from various electrolytes by both DCD and PED techniques were studied and compared. The effect of pulse duty cycle on thickness, current efficiency and hardness reached

maximum values at 40% duty cycle and 50 Hz frequencies with average current density of 4 A dm^{-2}. The potentiodynamic polarization techniques, from the values PED deposited Zn–Ni obtained from electrolyte-4 having higher corrosion resistance than other electrolyte samples. Although, 88:12% of Zn–Ni alloy coating on AISI 347 aircraft material having better structural, hardness and corrosion resistance.

Acknowledgement

This research was supported by the Collaborative Research Program among industry, academia and research institutes through the Korea Industrial Technology Association (KOITA) funded by the Ministry of Education, Science and Technology (KOITA-2011).

References

[1] W. Tian, F.Q. Xie, X.Q. Wu, Z.Z. Yang, Surf. Interface Anal. 41 (2009) 251–254.
[2] H.Y. Zheng, M.Z. An, J. Alloys Compd. 459 (2008) 548.
[3] S. Mohan, V. Ravindran, B. Subramanian, G. Saravanan, Trans. Inst. Met. Finish. 87 (2009) 85–89.
[4] L.M. Changa, D. Chena, J.H. Liub, R.J. Zhangb, J. Alloys Compd. 479 (2009) 489–493.
[5] R. Ramanauskas, L. Gudaviciute, A. Kalinicenko, R. Juskenas, J. Solid State Electrochem. 9 (2005) 900.
[6] M. Benballa, L. Nils, M. Sarret, C. Muller, Surf. Coat. Technol. 123 (2000) 55–61.
[7] I. Brooks, U. Erb, Scripta Mater. 44 (2001) 853–858.
[8] E. Chassaing, R. Wiart, J. Electrochim. Acta. 37 (1992) 545–553.
[9] S.E. Hadian, D.R. Gabe, Surf. Coat. Technol. 122 (1999) 118.
[10] S.H. Ashassi, A. Hagraha, A.N. Parvini, J. Manzooric, Surf. Coat. Technol. 140 (2001) 278.
[11] H.L. Seet, X.P. Li, W.C. Ng, H.Y. Chia, H.M. Zheng, K.S. Lee, J. Alloys Compd. 449 (2008) 279.
[12] R.M. Gnanamuthu, C.W. Lee, Mater. Sci. Eng. B 176 (2011) 1329.
[13] R.M. Gnanamuthu, C.W. Lee, J. Alloys Compd. 509 (2011) 8933.
[14] G. Saravanan, S. Mohan, Corros. Sci. 51 (2009) 197–202.
[15] E. Toth-Kadar, I. Bakonyi, L. Pongany, A. Cziraki, Surf. Coat. Technol. 88 (1996) 57.
[16] K. Haug, T. Jenkins, J. Phys. Chem. B 104 (2000) 10017–10023.
[17] M. Haichuan, S. Jin, R.Y. Lin, J. Electrochem. Soc. 150 (2003) C67.
[18] T. Pearson, J.K. Dennis, J. Appl. Electrochem. 20 (1990) 196–208.